Research Article

Journal of PeptideScience

Received: 12 July 2009 Revised: 11 July 2010 Accepted: 12 July 2010 Published online in Wiley Online Library: 2 September 2010

(wileyonlinelibrary.com) DOI 10.1002/psc.1284

Interactions of amyloid Aβ(1–42) peptide with self-assembled peptide nanospheres

Evan M. Smoak, Melanie P. Dabakis, Marsiyana M. Henricus, Robert Tamayev and Ipsita A. Banerjee*

In this work we have probed the interactions of the amyloid Aβ(1–42) peptide with self-assembled nanospheres. The nanospheres were formed by self-assembly of a newly developed bolaamphiphile bis(*N*-alpha-amido-methionine)-1,8 octane dicarboxylate under aqueous conditions. It was found that the interactions of the Aβ(1–42) peptide with the nanospheres were concentration as well as pH dependent and the peptide largely adopts a random coil structure upon interacting with the nanospheres. Further, upon incorporation with the nanospheres, we observed a relative diminution in the aggregation of Aβ(1–42) at low concentrations of Aβ(1–42). The interactions between the nanospheres and the Aβ(1–42) peptide were investigated by atomic force microscopy, transmission electron microscopy, circular dichroism, FTIR and fluorescence spectroscopy, and the degree of fibrillation in the presence and absence of nanospheres was monitored by the Thioflavine T assay. We believe that the outcome from this work will help further elucidate the binding properties of Aβ peptide as well as designing nanostructures as templates for further investigating the nucleation and fibrillation process of Aβ-like peptides.

Supporting information may be found in the online version of this article

Keywords: amyloid; self-assembly; nanospheres; peptides

Introduction

The misfolding and aggregation of proteins such as α-synuclein, insulin, prion, glucagon, and β-amyloid have long been implicated in the pathology of degenerative diseases such as type II diabetes, Parkinsons, spongiform encephalopathy, Huntingtons, and Alzheimers [1–4]. In particular, aggregation of the amyloid (Aβ) peptide into β-sheets that eventually form senile plaques has been considered one of the hallmarks of the early stages of Alzheimer's disease [5–10]. Mitigation of the fibrillation process and a deeper understanding of the peptide folding mechanism is therefore a necessity. Recent studies carried out have examined the oligomerization of Aβ(1–42) and its Pro [19] alloform, wherein it was observed that the substitution of Phe [19] by Pro [19] blocked fibril formation of the [Pro19] Aβ(1–42) peptide [11]. Advances in photochemical cross-linking techniques, such as photoinduced cross-linking of unmodified proteins (PICUP) [12,13] have also greatly aided in the quantification of Aβ oligomer frequency distribution [14–16]. Much research has also been conducted on the interaction of the Aβ(1–42) peptide with lipids of varying charges, as several studies have shown that the primary target of Aβ(1–42) plaques is the lipid bilayer that constitutes the cell membrane [17–24]. Luminescent conjugated polyelectrolyte probes (LCPs), have proven to be another group of molecular probes that have aided in studying the conformations of Aβ(1–42) [25,26]. Recently, it was shown that LCPs could be used to differentiate various Aβ(1–42) conformations within fibrils of *in vitro* as well as *in vivo* formed amyloid deposits [27]. Towards a similar effect, time-resolved anisotropy measurements (TRAMS) have been carried out in order to elucidate the conformations of the aggregates of Aβ(1–42) at early stages of fibril formation [28]. Researchers have also designed novel β-sheet breaker peptides that bind to the normal conformations and destabilize the β-sheet-rich structures that eventually lead to the formation of amyloid plaques as a new therapeutic approach for blocking amyloid fibril formation. In some cases, the β-sheet breaker peptides were found to reverse amyloid beta induced toxicity in vitro [29–31].

Over the past few years, nanostructures are becoming popular materials to elucidate the binding interactions of various peptides including Aβ(1–42) [32–34]. For example, interactions of carbon nanotubes with peptides have been examined for fabricating carbon nanotube-based protein binding devices [35,36]. Binding interactions of Au nanoparticles with amyloid fibrils have been shown to dissolve amyloid plaques through microwave radiation [37]. Co-polymeric nanoparticles of *N*-isopropylacrylamide:*N*-*tert*-butylacrylacrylamide (NiPAM : BAM), with different hydrophobicities have been shown to affect the nucleation step of Aβ(1–42) fibrillation [38], although the elongation process was mostly unaffected by the nanoparticles. Further, it was shown that the fibrillation of Aβ(1–42) initiated in the absence of those nanoparticles could be reversed by adding nanoparticles up to a certain time until mature fibrils appeared. PEGylated phospholipid nanomicelles, hybrids of Aβ(10–35)-PEG block co-polymers and

* *Correspondence to: Ipsita A. Banerjee, Department of Chemistry, Fordham University, 441 East Fordham Road, Bronx, NY 10458, USA.*
E-mail: banerjee@fordham.edu

Department of Chemistry, Fordham University, 441 East Fordham Road, Bronx, NY 10458, USA

Journal of PeptideScience

various amphiphilic surfactants have also been prepared to investigate the fibrillation process and as possible sources for mitigation of fibrillation of Aβ(1–42) [39–41]. The influence of hydrogenated and fluorinated nanoparticles on Aβ(1–40) secondary structures has also been examined [42]. It was found that while fluorinated nanoparticles induced α-helix structure in Aβ, their hydrogenated analogues lead to β-sheet formation and aggregation. Thus, while certain nanoparticles can be utilized as drugs to inhibit or reduce fibrillar aggregates, some nanoparticles have promoted fibril assembly [43,44]. For example, it has been shown that in some cases nanoparticles could enhance the likelihood of appearance of a critical nuclei that may be fibrillation-competent for homogeneous nucleation and augment the formation of protein clusters, thereby enhancing fibrillation as seen in the case of β_2-microglobulin in the presence of NiPAM : BAM nanoparticles [45,46]. Similarly, enhanced increased fibrillation has also been observed in the presence of TiO_2 nanoparticles [47].

Although significant research has been conducted with lipids, polymer-based nanoparticles, surfactants as well as metal or metal oxide nanoparticles relatively less information is available for studies related to interactions with peptide-based nanomaterials. Studies have shown that the Aβ peptide has a tendency to form exceedingly strong non-covalent bonds with surrounding peptides in the cerebral environment because of the close proximity of the polypeptide chains [48]. Further, *in situ*, close alignment of those peptide chains may be hampered by the natural interference of other proteins typically found in the cerebral environment, strongly suggesting that such proteins play a crucial role in the conformational structures of amyloid peptides *in vivo* and consequently may also affect the neurotoxic and cytotoxic properties of amyloid deposits.

In this work, we have examined the interactions of self-assembled peptide nanospheres with Aβ(1–42) in order to determine the efficacy in mitigating the aggregation of Aβ(1–42). The nanospheres were formed using a newly synthesized peptide bolaamphiphile bis(*N*-alpha-amido-methionine)-1,8 octane dicarboxylate. The purpose of using peptide nanostructures is to mimic the proteins surrounding the Aβ peptide in the cerebral environment. It is well known that oxidation of methionine considerably deters the rate of fibril formation in Aβ(1–42) [49]. Thus, it would be interesting to study the effects of nanostructures containing the methionine moiety on Aβ(1–42) conformation and investigate its effects on retarding the fibrillation process. In general, peptide nanostructures are known to be highly biocompabile [50] and the advantage of using nanostructures self-assembled from peptide bolaamphiphiles is the facile self-assembly mechanism and the resultant architectures formed can be controlled by varying external conditions [51,52]. Here in, we have investigated the effect of pH and concentration in order to better understand the mechanism of interactions of the nanospheres with Aβ(1–42), as well as the potential of the nanospheres in reducing the formation of aggregates and perhaps consequently reducing fibrillation. The interactions were probed by circular dichroism (CD), TEM, AFM analyses, fluorescence, FTIR spectroscopy, and Thioflavine T (ThT) assay.

Experimental

Materials

Aβ(1–42) peptide was purchased from American Peptide Company, Inc. lot R07010T1.*N*-(3-dimethylaminopropyl)-*N*-ethylcarbodiimide (EDAC), L-Methionine-methyl ester hydrochloride, sebacic acid, *N*-hydroxysuccinimide (NHS), dimethylformamide (DMF), DMSO, hexafluoroisopropanol (HFIP), DMSO-d6 with 0.1% v/v TMS, methanol, ThT, NIR-664-*N*-succinimidyl ester (NIR), and acetone were purchased from Sigma Aldrich. Buffer solutions of various pH, NaOH pellets, and HCl were purchased from Fisher Scientific. The compositions of the various buffer solutions at various pH were as follows: pH 4, potassium hydrogen phthalate; pH 5, potassium acid phthalate, sodium hydroxide; pH 6, potassium phosphate monobasic/sodium hydroxide; pH 7, phosphate monobasic/sodium hydroxide; pH 8, potassium phosphate monobasic/sodium hydroxide. The solvents were used as received.

Methods

Synthesis of Bis(*N*-Alpha-Amino-Methionine)-1,8 Octane Dicarboxylate

The bolaamphiphile bis(N-α-amido-methionine)-1,8 octane dicarboxylate was synthesized by modification of previously established methods [53,54]. Briefly, the reaction involved coupling the methionine methyl ester with sebacic acid in DMF solvent at 0 °C. EDAC was used as a coupling agent, whereas 1-hyrdoxybenzotriazole (HOBT) was used as an additive. The intermediate formed was then subjected to base hydrolysis in the presence of 0.1 M NaOH at 80 °C for removal of the protecting group. The product obtained (59% yield) was washed with a mixture of ice water and acetone, and yielded an off-white colored powder and recrystallized from 50 : 50 mixture of methanol and water. The ^{1}H NMR spectra were recorded with a Bruker 300 MHz NMR spectrometer. The ^{1}H NMR DMSO-d6 spectrum showed peaks at δ 1.3 (m, 8H) ($-CH_2$ groups); 2.1 (m, 14H) ($-CH_2$ and $-CH_3$ groups); 2.6 (t, 4H) ($-CH_2$ groups); 4.6 (d) (2H) (–CH group); 8.1 (s) due to hydrogen from the amide peaks. The elemental analysis of the compound revealed the following mass% C 51. 2; H 7. 1; N 5.32; O 21.82; S 14.56.

Self-Assembly of Nanospheres

Individual stock solutions of the bis(*N*-α-amido methionine)1, 8-octane dicarboxylate monomer were prepared in separate vials containing buffer solutions (0.2 M) at a pH range 4–9. The concentration of the monomer was kept constant at 1 mM. The samples were allowed to self-assemble for a period of 7–10 days at room temperature. The assemblies were sonicated (30 min), washed with distilled water and centrifuged at 14 000 rpm. Each sample was washed at least thrice before further analysis. After centrifugation and washing, the self-assembled nanospheres were dried and weighed. Assuming 100% conversion of precursor of known concentration, to nanospheres, we calculated the yield to be approximately 43.5%.

Preparation of Aβ(1–42) Peptide Solution

Dry Aβ(1–42) peptide was weighed and dissolved in HFIP to prepare a solution of 1 mg/ml^{-1} concentration. Aliquots were evaporated under vacuum in a speedvac. The evaporated Aβ(1–42) was stored at -20 °C until further use. Samples were then re-dissolved in DMSO and diluted 1 : 10 with 0.2 M buffer solutions (pH 4–9) and shaken in a water bath containing ice for 20 min. The solutions were then centrifuged, and the supernatants were used for further experiments.

Preparation of Nanosphere Bound Aβ(1–42)

Because higher yields of nanospheres were obtained upon self-assembly of the bolaamphiphile at pH 8, we used those nanospheres for analysis with the Aβ(1–42) peptide. Further, those nanospheres were washed thrice before incubation with the Aβ(1–42) peptide solutions. Varying amounts of Aβ(1–42) were added to the nanospheres, such that the final concentration of Aβ(1–42) in the mixture ranged from 10 to 100 μM (10, 20, 30, 50, 100 μM). Briefly, to each vial containing 500 μl of nanosphere solutions at a pH range 4–9, appropriate amounts of Aβ(1–42) peptide were added. In general, the samples were incubated and left on a shaker for a period of 72 h at 4 °C. The samples were shaken mildly during the incubation period, and then centrifuged to remove any unattached Aβ(1–42) that may be present in the supernatant and analyzed using various methods.

Preparation of Fluorescent Tagged of Aβ(1–42)

Fluorescent labeling has been utilized to probe protein binding in the past [55–57]. Here in, we tagged Aβ(1–42) with NIR dye in order to examine the binding process with nanospheres by fluorescence spectroscopy. The solution of NIR-664-*N*-succinimidyl ester (0.05 mM) was allowed to react with Aβ(1–42) solution (5 μM) and vortexed overnight at 3.9 °C. The sample was then centrifuged at 15 000 × g for 30 min and washed with distilled water twice before further analysis.

ThT Binding Assay

The degree of Aβ(1–42) fibrillization was determined using the fluorescent dye, ThT, which specifically binds to fibrillar conformations [58,59]. Samples were prepared as described above with final Aβ(1–42) concentration of 30 μM. After incubation with nanospheres for 72 h, 200 μl of ThT was added to each test sample to a final concentration of 5 μM. Samples were shaken for 60 s prior to each measurement. Relative fluorescence intensity was measured using Jobin Yvon Fluoromax 3 fluorescence spectrometer. Measurements were performed at an excitation wavelength of 437 nm and an emission of 480 nm (pre-determined experimentally). To account for background fluorescence, fluorescence intensity from control solution without Aβ(1–42) was subtracted from solution containing Aβ(1–42).

Characterization

Transmission electron microscopy

Samples were washed twice with distilled water and air-dried onto carbon-coated copper grids for characterization by transmission electron microscopy (TEM) (JEOL 1200 EX) operated at 100 kV. The Aβ(1–42) incorporated samples with and without nanospheres were negatively stained with 0.5% w/v uranyl acetate before analysis.

Atomic force microscopy

The atomic force microscopy (AFM) was carried out using a Quesant Universal SPM instrument in tapping mode in air using a silicon–nitride cantilever. Samples were washed twice with distilled water and then deposited on the surface of a glass slide and air-dried. The resultant, dried samples were then analyzed by AFM. For AFM analysis, sample nanosphere solutions incubated with 10 μl Aβ(1–42) were used.

Particle sizing using dynamic light scattering analysis (DLS)

A NICOMP 380 ZLS zeta potential/particle sizer system (Santa Barbara, California, USA) was used to determine the sizes of the samples. DLS measurements were carried out at 25 °C and at a pH range 4–8. The concentrations of the suspensions were adjusted within the operational limits of the instrument and the suspension pH was adjusted by the addition of standard buffer solutions.

FTIR spectroscopy

In order to confirm the incorporation of Aβ(1–42) onto the nanospheres FTIR analyses were carried out using Matteson Infinity IR equipped with DIGILAB, ExcaliBuv HE Series FTS 3100 software. The samples were dried in vacuum at 30 °C and -635 mm Hg and mixed with KBr to make pellets, and then analyzed. All spectra were taken at 4 cm^{-1} resolution with 100 scans taken for averaging. Sample measurements were carried between 400 and 4000 cm^{-1}.

CD spectroscopy

CD measurements were carried out using a JASCO J-720 spectropolarimeter. Samples were scanned at least five times at the rate of 200 nm min^{-1} with a 0.5 nm step, 1 nm bandwidth, and then averaged. To obtain the critical molar ratio for optimal binding of the nanospheres with Aβ(1–42) different concentrations of Aβ(1–42) were added to the nanospheres at varying pH. In the experiments, a blank run made with buffer alone was subtracted from the experimental spectra for correction. Further, the CD spectra of nanospheres alone were measured, and the spectra of the nanospheres alone were subtracted from the samples containing Aβ(1–42) with nanospheres. The 190–250 nm spectra were used for analysis. All the spectra were smoothed and converted to the mean residue ellipticity [θ] in deg*cm^2/dmol.

Fluorescence spectroscopy

Fluorescence spectra were obtained using a Jobin Yvon Fluoromax 3 fluorescence spectrometer. All measurements were carried out in aqueous solutions using quartz cuvettes. A reference cuvette holding the solvent was used for baseline correction purposes. NIR labeled Aβ(1–42) at a concentration of 30 μM was incubated with the nanospheres in buffer solutions of varying pH values for a period of 48–72 h in a water bath at 37 °C, after which fluorescence spectra of the samples were obtained. Control experiments were conducted using the NIR labeled Aβ(1–42) as well as the NIR solution.

Results and Discussion

In order to mimic biological assemblies such as liposomes, peptide assemblies, and channel proteins, many peptide-based nano and microstructures have been studied thus far [60–65]. It has been observed that such assemblies are mostly formed due to non-covalent interactions or protonation and/or hydrophobic interactions between the peptide moieties either instantaneously or over a period of time [66,67]. Here in, we have synthesized a new bolaamphiphile, HOOC–Met–NH–CO–$(CH_2)_8$–NH–CO–Met–COOH. For this study, the alkyl spacer between the amino acid head groups was limited to eight methylene groups. The effect of variation of chain length on the self-assembly process is being currently studied and will be reported separately.

Journal of PeptideScience

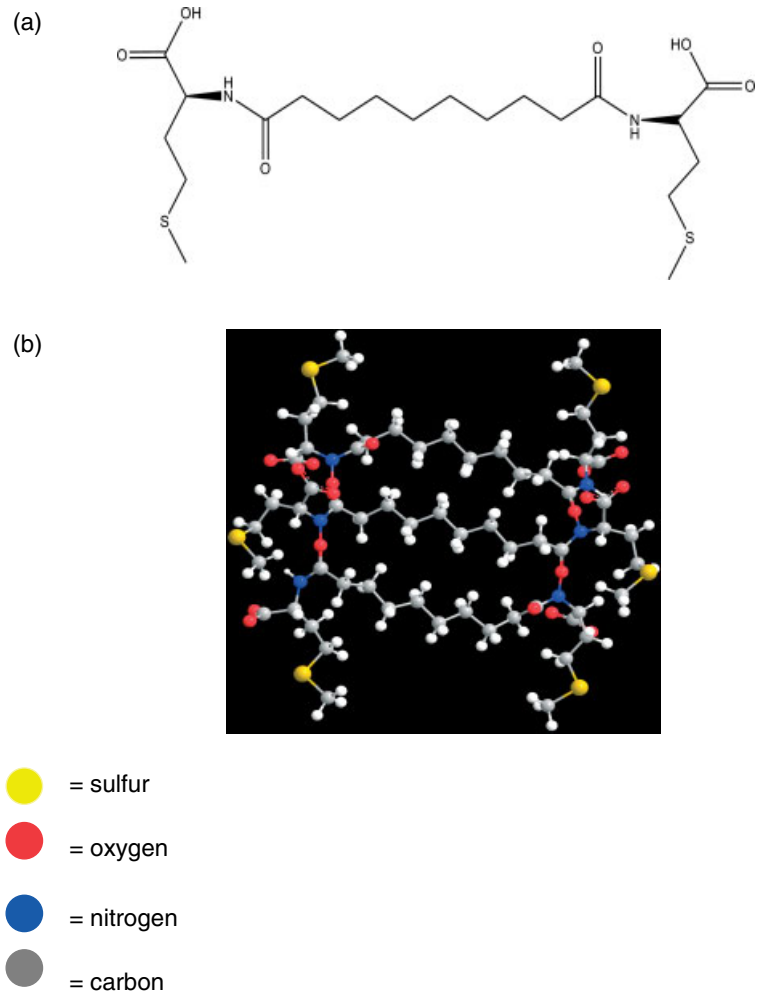

Figure 1. (A) Chemical structure of methionine bolaamphiphile synthesized; (B) proposed three-dimensional model for self-assembly of the nanospheres.

After synthesis, the bolaamphiphile was dispersed in solutions of pH 4–9 for self-assembly of the nanostructures. In general, a mixture of nanospheres and nanotubular assemblies were observed at lower pH, whereas mainly spherical assemblies were formed at pH>6. This is mainly due to the difference in hydrogen bonding patterns involved in the self-assembly of the nanostructures. At low pH, in addition to hydrogen bonding interactions between the NH-amide and carbonyl groups, hydrogen bonding is also expected between the carboxyl groups leading to nanotubular structures [66,67]. While at higher pH, when the carboxyl groups are deprotonated, hydrogen bonding is relatively less leading to the formation of spherical nanostructures. The chemical structure of the bolaamphiphile synthesized as well as the proposed three-dimensional model are shown in Figure 1(A) and (B), respectively. For the purposes of studying interactions with the Aβ(1–42) peptide, we used nanospheres, which were self-assembled at pH 8, because higher yields of nanospheres were obtained under those conditions. Once self-assembled, the nanospheres were sonicated, centrifuged, washed and were found to be stable in aqueous solutions at room temperature for several months. It is most likely that the nanostructures are formed primarily due to hydrogen bonding interactions between the C═O groups and the – NH groups of the amide moieties of the bolaamphiphile.

Interactions of Nanospheres with Aβ(1–42)

Atomic force microscopy and dynamic light scattering

In order to study the interactions of the nanospheres with Aβ(1–42) AFM analyses were conducted at pH range 4–8. In general, the self-assembled nanospheres alone had a diameter of 200–300 nm before incubation with the Aβ(1–42) as shown in Figure 2(A), whereas Figure 2(B) shows the AFM topography image of the nanospheres alone. We observed that a change in the diameter occurred over the course of 72 h after incubation with the Aβ(1–42) sequence and leveled off after approximately 72 h at a size range approximately 400–600 nm depending upon the sizes of the nanospheres. This was confirmed by DLS analsyis (Figure 3(A)). The increase in sizes upon incubation with Aβ(1–42) is indicative of incorporation of the Aβ(1–42) onto the surface of the nanospheres. This increase in size was observed to be greatest at a pH range 4–7, which is likely due to the relatively higher degree of hydrogen bonding interactions at lower pH as opposed to higher pH. Figure 3(B) and (C) shows the three-dimensional AFM images of the nanospheres at pH 5 before and after 72 h of incubation with Aβ(1–42) at higher concentration (when 50 μM concentration of Aβ(1–42) was used). The roughened surface of the nanospheres (Figure 3(B)), compared with regular nanospheres (as seen in the 3D AFM image, Figure 3(A)) strongly suggests that the Aβ(1–42) is incorporated onto the nanospheres.

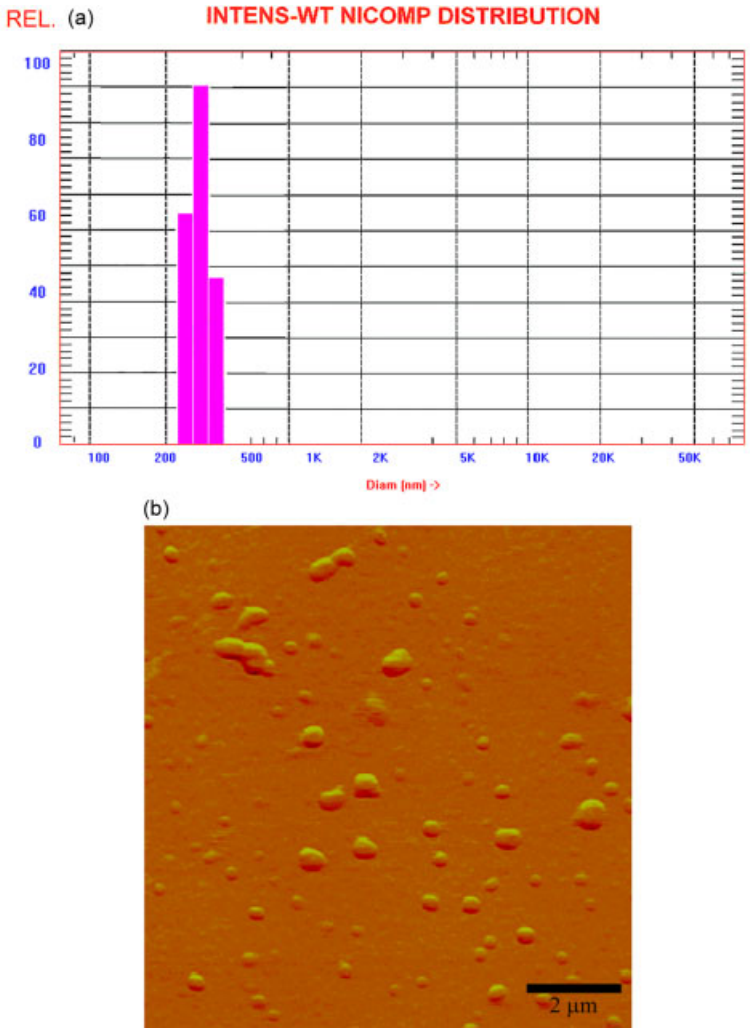

Figure 2. (A) DLS analysis of nanospheres formed at pH 8; (B) AFM topography image of nanospheres formed at pH 8. This figure is available in colour online at wileyonlinelibrary.com/journal/jpepsci.

Further, at those concentrations it appears that binding of Aβ(1–42) to the nanospheres, may lead to the change in the conformation of the peptide. We also carried out AFM analysis at lower concentrations (data not shown), which showed similar trends, although the increase in roughness and relative height was proportional to the concentration of the Aβ(1–42) used.

Transmission Electron Microscopy

TEM analyses were also used to probe the interactions of Aβ(1–42) with the nanospheres at varying pH. Figure 4(A) shows the TEM images obtained before incubation with Aβ(1–42) showing nanospheres ranging from 200 to 300 nm in diameter, which corroborates the sizes of the nanospheres observed using the AFM and DLS analyses. Figure 4(B) shows the TEM image of the nanospheres examined after 72 h of incubation with Aβ(1–42) at low concentration (20 µM at pH 7), whereas Figure 4(B) shows the TEM image obtained after incubation with Aβ(1–42) (50 µM at pH 7) and Figure 4(C) shows the TEM image obtained when the nanospheres were incubated with Aβ(1–42) (100 µM concentration) at pH 7. As seen from Figure 4(B), it appears that the Aβ(1–42) tends to accumulate around the periphery of the nanospheres further confirming that the nanospheres were capable of interacting with the Aβ(1–42) sequence. Another aspect was that at higher concentration, the nanospheres were completely covered with the peptide, however upon incubation with much higher concentrations of Aβ(1–42) sequence (100 µM), although the nanospheres bound to Aβ(1–42), some fibrils were also observed, although lesser than those observed in the absence of nanospheres (Figure 4(E)). This is perhaps due to the fact that at high concentrations of Aβ(1–42) the binding sites of the nanospheres are already saturated, and there may be an increase in the local concentration of the peptide leading to formation of fibrils at higher concentrations. Overall, we observed that upon addition of the nanospheres relatively less fibrillation of the Aβ(1–42) was observed after a period of 72 h between pH 4 and pH 7 particularly at lower concentrations, when compared to the growth of Aβ(1–42) peptide in the absence of nanospheres (Figure 4(E)). It is to be noted that regardless of the concentration, fibrillation was relatively less, compared to Aβ(1–42) alone. These results indicate the nanospheres are capable of not only binding with the Aβ(1–42) but may also mitigate fibrillation of the Aβ(1–42) at appropriate concentrations. The TEM image shown in Figure 4(B) strongly suggests that Aβ(1–42) most likely binds to the nanospheres in the early stages of oligomer formation and once its bound to the

Journal of PeptideScience

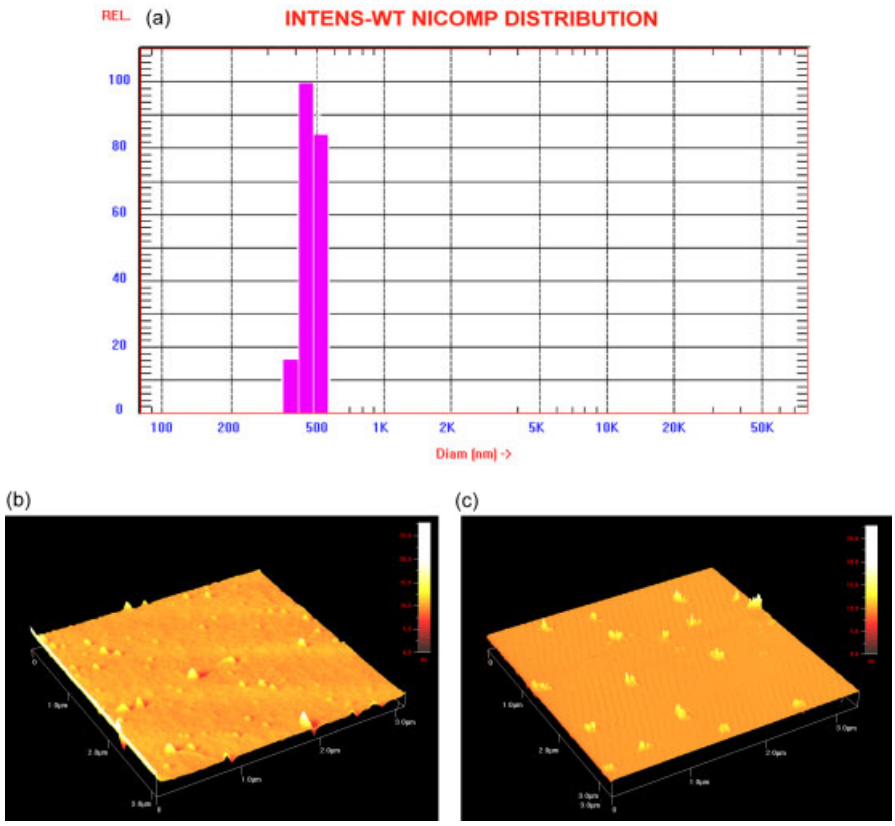

Figure 3. (A) DLS analysis of Aβ(1–42) incorporated nanospheres at pH 6 after 72 h of incubation; (B) comparison of 3D AFM images of nanospheres before and after binding with Aβ(1–42) at pH 6 after 72 h. This figure is available in colour online at wileyonlinelibrary.com/journal/jpepsci.

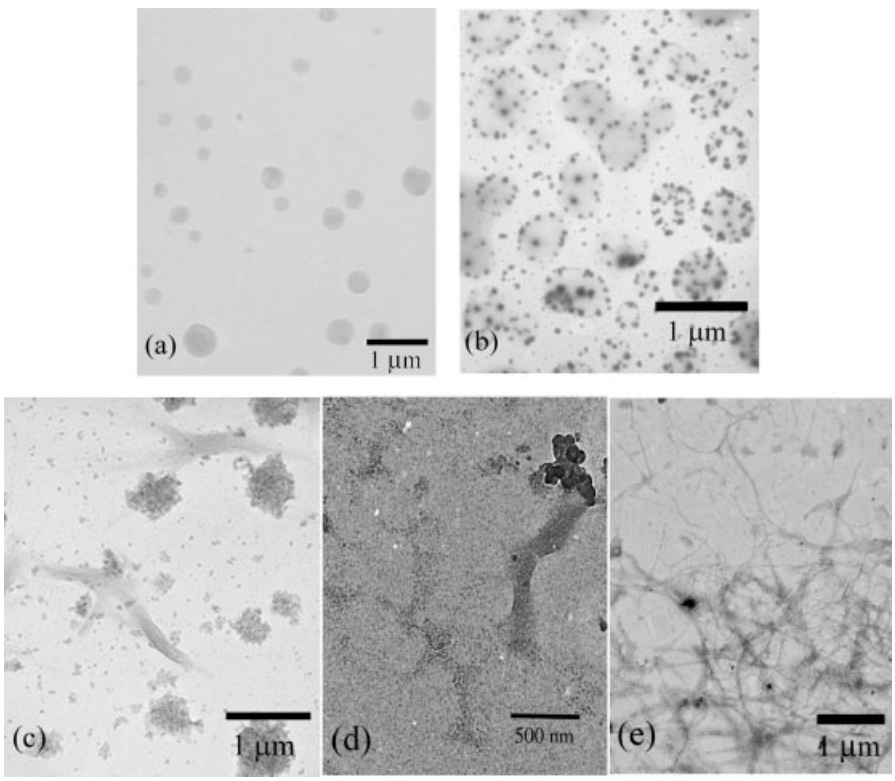

Figure 4. (A) TEM image of nanospheres; (B) nanospheres bound to Aβ 1–42) after 72 h of incubation at pH 7 at 20 µM Aβ(1–42) concentration; (C) nanospheres bound to Aβ(1–42) after 72 h of incubation at pH 7 at 50 µM Aβ(1–42) concentration; (D) nanospheres bound to Aβ(1–42) after 72 h of incubation at pH 7 at 100 µM Aβ(1–42) concentration; (E) fibril formation of Aβ(1–42) (50 µM) in the absence of nanospheres at pH 7 after 72 h.

nanospheres, further formation of protofibrils and fibrils is slowed down.

FTIR Analysis

In order to further confirm the incorporation of the Aβ peptide onto the nanospheres, the samples were also analyzed by FTIR spectroscopy. Figures 5(A)–(C) shows the comparison of IR spectra of Aβ(1–42), Aβ(1–42) (30 μM) incorporated onto the nanospheres, and neat nanospheres, respectively. The spectra illustrate the data obtained at pH 6. As the samples were dried prior to FTIR analysis, it is probable that the local concentration of the peptide may be relatively higher, which may further influence the secondary structural transformation. The amide I region (1600–1700 cm^{-1}), of Figure 5(A), Aβ(1–42) alone shows, a peak at 1627 cm^{-1} due to amide I stretching indicative of a β-sheet structure [68]. Upon binding to the nanospheres, as shown in Figure 5(B), we observed a shift in the amide I stretching vibration peaks to 1638 and 1647 cm^{-1} (indicative of random coil conformations) and 1652 cm^{-1}, are also observed. This is most likely due to interactions between the nanospheres and the Aβ(1–42), which may have lead to a change in the conformation. In addition, the peak at 1627 cm^{-1} is diminished, indicating a reduction in the β-sheet structure. The peaks at 1652, 1683, and 1670 cm^{-1} observed, matches those of the nanospheres alone (Figure 5(C)). Additional peaks observed in lower 1600 cm^{-1} region for the nanospheres are diminished upon binding to the Aβ (1–42) peptide.

Circular Dichroism

It is well known that peptide misfolding is one of the major causes of amyloid plaque formation in amyloidogenic diseases such as Alzheimer's disease [69–72]. CD spectra in the UV region were used to monitor changes in the secondary structure. Figure 6 shows the CD spectra of Aβ(1–42) in the presence and absence of the self-assembled nanospheres at pH values ranging from 4 to 8 after incubation for 72 h. Before the CD measurement, in order to determine the critical molar ratio for Aβ(1–42) binding with the nanospheres a pre-experiment was carried out where in the nanosphere to Aβ ratio of about 35 was obtained. Thus, for measurements at all pH, we chose 50 as the actual nanosphere to Aβ ratio to ensure the presence of enough nanospheres. In general, in the presence of the nanospheres, a change in the CD spectrum was observed. It appears that in the presence of nanospheres, mostly random coil structures are formed. At pH 4–6, a negative maxima is observed around 195 nm, showing random coil conformation in the presence of nanospheres, whereas in the absence of nanospheres, at pH 4 the spectrum shows a mix of random coil and β-sheet structure. At pH 6 however, in the absence of the nanospheres the structure largely represents a β-sheet structure, where as upon interacting with the nanospheres, it exhibits a random coil structure. At pH 8, in the absence of the nanospheres, the spectrum obtained shows also shows a β-sheet-like structure however, in the presence of the nanospheres, the spectrum observed appears to be that of random coil, although not as distinct as those observed in the pH range 4–6. The results of the CD analyses show that Aβ(1–42) undergoes conformation changes at varying pH, confirming the interactions with the nanospheres.

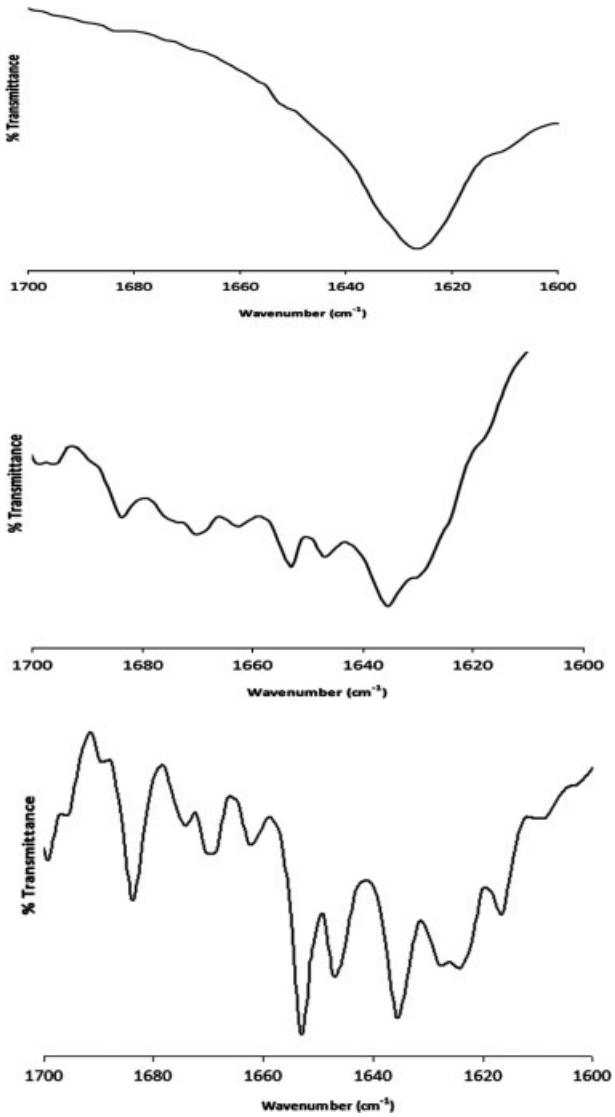

Figure 5. Comparison of FTIR spectra of (A) Aβ(1–42); (B) Aβ(1–42) bound to nanospheres; (C) Self-assembled nanospheres.

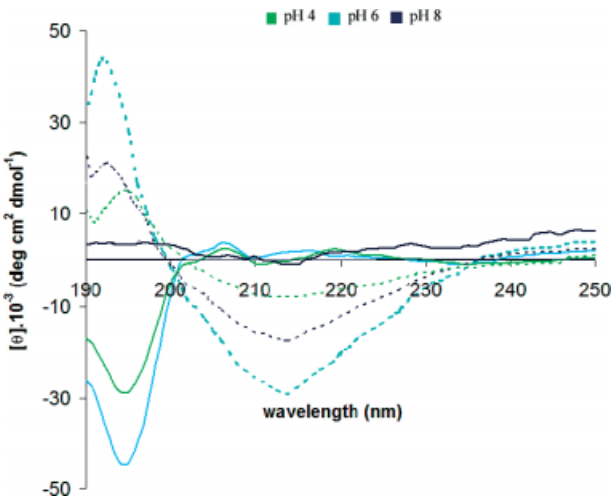

Figure 6. Comparison of CD spectra of Aβ(1–42) in the presence and absence of nanospheres (- - - -) indicates Aβ(1–42) and (———) indicates Aβ(1–42) in the presence of nanospheres.

Journal of PeptideScience

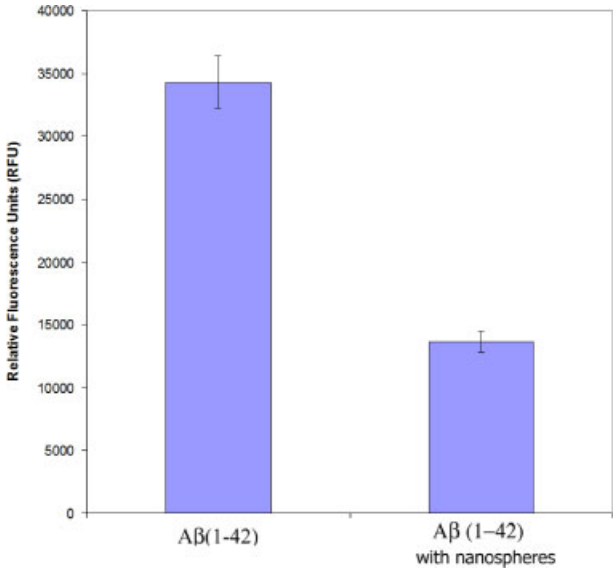

Figure 7. Effect of nanospheres on Aβ(1–42) (20 μM) aggregation by ThT assay at pH 7. Increase in relative fluorescence units (RFU) is proportional to fibril formation. Error bars indicate standard deviation. This figure is available in colour online at wileyonlinelibrary.com/journal/jpepsci.

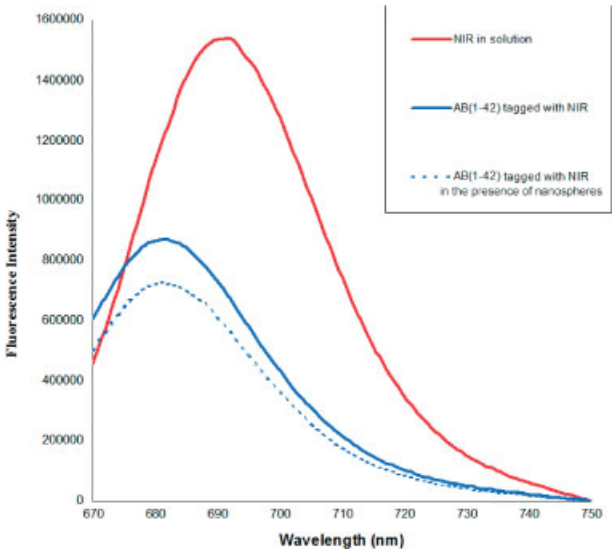

Figure 8. Comparison of fluorescence spectra of Aβ(1–42) in solution and before and after incorporation of nanospheres at pH 6.

ThT Assay

For determining the effect of amyloid aggregation process in the presence of the nanospheres, we used the ThT interaction assay as a more definite deterministic method. In general, amyloid protein fibrils possess specific dye binding properties due to their characteristic fibrillar conformations. It is well known that binding of ThT to amyloid fibrils causes enhancement of ThT fluorescence [73], thus we conducted a ThT assay for determination of fibril formation in the presence and absence of nanospheres. In general, the relative fluorescence intensity was lesser for the nanosphere treated samples. As shown in Figure 7, ThT fluorescence spectroscopic assay showed a reduction in the relative fluorescence intensity of nanosphere treated sample to less than half of that compared to the untreated control, indicating significant mitigation of β-sheeted fibril formation in nanosphere treated samples. The figure shown is that obtained at pH 7. A similar effect was observed at other pH as well, athough at pH 8, the difference was not as significant.

Fluorescence Studies

To explore the interactions of the Aβ(1–42) peptide with the nanospheres, we examined the fluorescence changes observed, when fluorescent-labeled Aβ(1–42) was incubated with the nanospheres. The highly fluorescent NIR-664 succinimide ester was covalently coupled to the *N*-terminal residue of Aβ(1–42) before studies were carried out. Figure 8 shows the fluorescence spectra at 37 °C obtained at pH 6. First, the covalent binding of NIR to Aβ(1–42) was confirmed, by comparing the fluorescence spectra of the dye in solution with that of Aβ(1–42) second, the coupling reaction was carried out and the unreacted dye was removed. We observed a blue shift of the fluorescence maxima from 689 to 682 nm, as well quenching in the fluorescence, confirming that Aβ(1–42) was tagged with NIR. Further, upon binding to the nanospheres additional fluorescence quenching, was observed along with a blue shift to 680 nm. In general, similar quenching was observed at a pH range 4–7. Quenching at higher pH was relatively less, signifying that there was relatively less interactions between Aβ(1–42) and the nanospheres at higher pH. This is likely due to the fact that the pI of Aβ(1–42) is 5.37 and hence at pH 8 Aβ(1–42) would be deprotonated [74]. In addition, due to the negative charge of the deprotonated state of the carboxylate moieties of the nanospheres at high pH, the interactions are likely to be relatively less at higher pH. Thus, at high pH there would most likely be repulsion between the nanospheres and the Aβ(1–42). Therefore, one can conclude that a pH range 4–7 is likely ideal for the purposes of facilitating the binding interactions between the nanospheres and Aβ(1–42).

Conclusions

In this work we have developed a new peptide bolaamphiphile, which upon self-assembly formed nanospheres. Those nanospheres were capable of non-covalently interacting with the Aβ(1–42) peptide in a pH sensitive manner. In general, we found that at a pH range 4–7, the interactions with Aβ(1–42) peptide were relatively stronger. Further, upon incorporation to the nanospheres, we observed that there was a relative retardation in the aggregation of Aβ(1–42) over a pH range 4–7 in the presence of low concentrations of Aβ(1–42) ($\leq$30 μM). Further studies are ongoing to develop tailored peptide-based nanostructures for efficient interactions with a wide range of peptides to manufacture an array of nanostructures, explicitly capable of binding to specific peptide moieties. Further verification of the *in vivo* effects of the nanospheres is still under investigation. We believe that the outcome from this work will enable us to further elucidate the mechanism by which beta-amyloid fibrillization occurs as well as designing nanostructures as templates for molecular therapeutics in the retardation of Aβ(1–42) aggregate formation implicated in many neurodegenerative disease pathologies.

Acknowledgements

The authors thank Dr Areti Tsiola and Dr Karl Fath at the Queens College (CUNY) Core Facilities for Imaging, Cell and Molecular

Biology for the use of the TEM. ES thanks the Fordham University Summer Science Internship Program for financial support. IB thanks the Fordham University faculty Research Grant for financial support.

Supporting information

Supporting information may be found in the online version of this article.

References

1 Conway KA, Harper JD, Lansbury PT, Jr. Fibrils formed in vitro from α-synuclein and two mutant forms linked to Parkinson's disease are typical amyloid. *Biochemistry* 2000; **39**: 2552–2563.
2 Smith DP, Tew DJ, Hill AF, Bottomley SP, Masters CL, Barnham KJ, Cappai R. Formation of a high affinity lipid-binding intermediate during the early aggregation phase of α-synuclein. *Biochemistry* 2008; **47**: 1425–1434.
3 Stefani M, Dobson CM. Protein aggregation and aggregate toxicity: new insights into protein folding, misfolding diseases and biological evolution. *J. Mol. Med.* 2003; **81**: 678–699.
4 Forloni G, Terreni L, Bertani I, Fogliarino S, Invernizzi R, Assini A, Ribizzi G, Negro A, Calabrese E, Volenté MA, Mariani C, Franceschi M, Tabaton M, Bertoli A. Protein misfolding in Alzheimer's and Parkinson's disease: genetics and molecular mechanisms. *Neurobiol. Aging* 2002; **23**: 957–976.
5 Yoda M, Miura T, Takeuchi H. Non-electrostatic binding and self-association of amyloid β-peptide on the surface of tightly packed phosphatidylcholine membranes. *Biochem. Biophys. Res. Commun.* 2008; **376**: 56–59.
6 Bokvist M, Lindström F, Watts A, Gröbner G. Two types of Alzheimer's β-Amyloid (1–40) peptide membrane interactions: aggregation preventing transmembrane anchoring versus accelerated surface fibril formation. *J. Mol. Biol.* 2004; **335**: 1039–1049.
7 Ha C, Park CB. Ex situ atomic force microscopy analysis of β-amyloid self-assembly and deposition on a synthetic template. *Langmuir* 2006; **22**: 6977–6985.
8 Kremer JJ, Sklansky DJ, Murphy RM. Profile of changes in lipid bilayer structure caused by β-amyloid peptide. *Biochemistry* 2001; **40**: 8563–8571.
9 Marko-Varga G, Fehniger TE. Proteomics and disease – the challenges for technology and discovery. *J. Proteome Res.* 2004; **3**: 167–178.
10 Koppaka V, Axelsen PH. Accelerated accumulation of amyloid β proteins on oxidatively damaged lipid membranes. *Biochemistry* 2000; **39**: 10011–10016.
11 Bernstein SL, Wyttenbach T, Baumketner A, Shea JE, Bitan G, Teplow DB, Bowers MT. Amyloid β-protein: monomer structure and early aggregation states of Aβ 42 and its Pro19 alloform. *J. Am. Chem. Soc.* 2005; **127**: 2075–2084.
12 Fancy DA, Denison C, Kim K, Xie YQ, Holdeman T, Amini F, Kodadek T. Scope, limitations and mechanistic aspects of the photo-induced cross-linking of proteins by water-soluble metal complexes. *Chem. Biol.* 2000; **7**: 697–708.
13 Fancy DA, Kodadek T. Chemistry for the analysis of protein-protein interactions: rapid and efficient cross-linking triggered by long wavelength light. *Proc. Natl. Acad. Sci. U.S.A.* 1999; **96**: 6020–6024.
14 Bitan G, Teplow DB. Rapid photochemical cross-linking – a new tool for studies of metastable, amyloidogenic protein assemblies. *Acc. Chem. Res.* 2004; **37**: 357–364.
15 Marina GB, Kirkitadze MD, Lomakin A, Vollers SS, Benedek GB, Teplow DB. Amyloid β-protein (Aβ) assembly: Aβ 40 and Aβ 42 oligomerize through distinct pathways. *Proc. Natl. Acad. Sci. U.S.A.* 2003; **100**: 330–335.
16 Bitan G, Lomakin A, Teplow DB. Amyloid β-protein oligomerization: prenucleation interactions revealed by photo-induced cross-linking of unmodified proteins. *J. Biol. Chem.* 2001; **276**: 35176–35184.
17 Wong PT, Schauerte JA, Wisser KC, Ding H, Lee EL, Steel DG, Gafni A. Amyloid-β membrane binding and permeabilization are distinct processes influenced separately by membrane charge and fluidity. *J. Mol. Biol.* 2009; **386**: 81–96.
18 Ikeda K, Matsuzaki K. Driving force of binding of amyloid β-protein to lipid bilayers. *Biochem. Biophys. Res. Commun.* 2008; **370**: 525–529.
19 Terzi E, Hölzemann G, Seelig J. Self-association of β-amyloid peptide (1–40) in solution and binding to lipid membranes. *J. Mol. Biol.* 1995; **252**: 633–642.
20 Salay. LC, Qi Wei, Keshet B, Tamm LK, Fernandez EJ. Membrane interactions of a self-assembling model peptide that mimics the self-association, structure and toxicity of Aβ-(1–40). *Biochim. Biophys. Acta (Biomembranes)* 2009; **1788**: 1714–1721.
21 Ambroggio EE, Kim DH, Separovic F, Barrow CJ, Barnham KJ, Bagatolli LA, Fidelio GD. Surface behavior and lipid interaction of Alzheimer β-amyloid peptide 1–42: a membrane-disrupting peptide. *Biophys. J.* 2005; **88**: 2706–2713.
22 Ji S-R, Wu Y, Sui S-F. Cholesterol is an important factor affecting the membrane insertion of β-amyloid peptide (Aβ 1–40), which may potentially inhibit the fibril formation. *J. Biol. Chem.* 2002; **277**: 6273–6279.
23 Gorbenko GP, Kinnunen PKJ. The role of lipid–protein interactions in amyloid-type protein fibril formation. *Chem. Phys. Lipids* 2006; **141**: 72–82.
24 McLaurin J, Chakrabartty A. Characterization of the interactions of Alzheimer β-amyloid peptides with phospholipid membranes. *Eur. J. Biochem.* 1997; **245**: 355–363.
25 Nilsson KPR, Herland A, Hammarström P, Inganäs O. Conjugated polyelectrolytes: conformation-sensitive optical probes for detection of amyloid fibril formation. *Biochemistry* 2005; **44**: 3718–3724.
26 Nilsson KP, Hammarström P, Ahlgren F, Herland A, Schnell EA, Lindgren M, Westermark GT, Inganäs O. Conjugated polyelectrolytes – conformation-sensitive optical probes for staining and characterization of amyloid deposits. *Chem. Bio. Chem.* 2006; **7**: 1096–1104.
27 Nilsson KPR, Åslund A, Berg I, Nyström S, Konradsson P, Herland A, Inganäs O, Stabo-Eeg F, Lindgren M, Westermark GT, Lannfelt L, Nillson LNG, Hammarström P. Imaging distinct conformational states of amyloid-β fibrils in Alzheimer's disease using novel luminescent probes. *ACS Chem. Biol.* 2007; **2**: 553–560.
28 Allsop D, Swanson L, Moore S, Davies Y, York A, El-Agnaf OMA, Soutar I. Fluorescence anisotropy: a method for early detection of Alzheimer β-peptide (Aβ) aggregation. *Biochem. Biophys. Res. Commun.* 2001; **285**: 58–63.
29 Adessi C, Soto C. Beta-sheet breaker strategy for the treatment of Alzheimer's disease. *Drug Dev. Res.* 2002; **56**: 184–193.
30 Chacón MA, Barria MI, Soto C, Inestrosa NC. β-Sheet breaker peptide prevents Aβ-induced spatial memory impairments with partial reduction of amyloid deposits. *Mol. Psychiatr.* 2004; **9**: 953–961.
31 Nakagami Y, Nishimura S, Murasugi T, Kaneko I, Meguro M, Marumoto S, Kogen H, Koyama K, Oda T. A novel compound RS-0466 reverses β-amyloid-induced cytotoxicity through the Akt signaling pathway in vitro. *Eur. J. Pharmacol.* 2002; **457**: 11–17.
32 Yokoyama K, Welchons DR. The conjugation of amyloid beta protein on the gold colloidal nanoparticles' surfaces. *Nanotechnology* 2007; **18**: 105101.
33 Lynch I, Dawson KA. Protein–nanoparticle interactions. *Nanotoday* 2008; **3**: 40–47.
34 Cabaleiro-Lago C, Quinlan-Pluck F, Lynch I, Dawson KA, Linse S. Dual effect of amino modified polystyrene nanoparticles on amyloid β protein fibrillation. *ACS Chem. Neurosci.* 2010; **1**: 279–287.
35 Zheng L, Jain D, Burke P. Nanotube–peptide interactions on a silicon chip. *J. Phys. Chem. C.* 2009; **113**: 3978–39851.
36 Zorbas V, Smith AL, Xie H, Ortiz-Acevedo A, Dalton AB, Diedkmann GR, Draper RK, Baughman RH, Musselman IH. Importance of aromatic content for peptide/single-walled carbon nanotube interactions. *J. Am. Chem. Soc.* 2005; **127**: 12323–12328.
37 Kogan MJ, Bastus NG, Amigo R, Grillo-Bosch D, Araya E, Turiel A, Labarta A, Giralt E, Puntes VF. Nanoparticle-mediated local and remote manipulation of protein aggregation. *Nano. Lett.* 2006; **6**: 110–115.
38 Cabaleiro-Lago C, Quinlan-Pluck F, Lynch I, Lindman S, Minogue AM, Thulin E, Walsh DM, Dawson KA, Linse S. Inhibition of amyloid β protein fibrillation by polymeric nanoparticles. *J. Am. Chem. Soc.* 2008; **130**: 15437–15443.
39 Pai AS, Rubenstein I, Önyüksel H. PEGylated phospholipid nanomicelles interact with β-amyloid(1–42) and mitigate its

Journal of PeptideScience

β-sheet formation, aggregation and neurotoxicity in vitro. *Peptides* 2006; **27**: 2858–2866.

40 Wang S, Chen YT, Chou SW. Inhibition of amyloid fibril formation of β-amyloid peptides via the amphiphilic surfactants. *Biochim. Biophys. Acta.* 2005; **1741**: 307–313.

41 Burkoth TS, Benzinger TLS, Urban V, Lynn DG, Meredith SC, Thiyagarajan P. Self-assembly of Aβ((10–35))-PEG block copolymer fibrils. *J. Am. Chem. Soc.* 1999; **121**: 7429–7430.

42 Rocha S, Thunemann AF, Pereira MDC, Coelho M, Mohwald H, Brezenski G. Influence of fluorinated and hydrogenated nanoparticles on the structure and fibrillogenesis of amyloid beta-peptide. *Biophys. Chem.* 2008; **137**: 35–42.

43 Triulzi RC, Dai Q, Zou J, Leblanc RM, Gu Q, Orbulescu J, Huo Q, Photothermal ablation of amyloid aggregates by gold nanoparticles. *Colloids Surf. B Biointerfaces* 2008; **63**: 200–208.

44 Fei L, Perrett S. Effect of nanoparticles on protein folding and fibrillogenesis. *Int. J. Mol. Sci.* 2009; **10**: 646–655.

45 Linse S, Cabaleiro-Lago C, Xue WF, Lynch I, Lindman S, Thulin E, Radford SE, Dawson KA. Nucleation of protein fibrillation by nanoparticles. *Proc. Natl. Acad. Sci. U.S.A.* 2007; **104**: 8691–8696.

46 Colvin VL, Kulinowski KM. Nanoparticles as catalysts for protein fibrillation. *Proc. Natl. Acad. Sci. U.S.A.* 2007; **104**: 8679–8680.

47 Wu WH, Sun X, Yu YP, Hu J, Zhao L, Liu Q, Zhao YF, Li YM. TiO_2 nanoparticles promote β-amyloid fibrillation in vitro. *Biochem. Biophys. Res. Commun.* 2008; **373**: 315–318.

48 Choo LP, Wetzel DL, Halliday WC, Jackson M, LeVine SM, Mantsch HH. In situ characterization of β-amyloid in Alzheimer's diseased tissue by synchrotron Fourier transform infrared microspectroscopy. *Biophys. J.* 1996; **71**: 1672–1679.

49 Hou L, Kang I, Marchant RE, Zagorski MG. Methionine 35 oxidation reduces fibril assembly of the amyloid aβ-(1–42) peptide of Alzheimer's disease. *J. Biol. Chem.* 2002; **277**: 40173–40176.

50 Spear RL, Tamayev R, Fath KR, Banerjee IA. Templated growth of calcium phosphate on tyrosine derived microtubules and their biocompatibility. *Colloids Surf. B. Biointerfaces* 2007; **60**: 158–166.

51 Hentschel J, Börner HG. Peptide-directed microstructure formation of polymers in organic media. *J. Am. Chem. Soc.* 2006; **128**: 14142–14149.

52 Hartgerink JD, Beniash E, Stupp SI. Peptide-amphiphile nanofibers: a versatile scaffold for the preparation of self-assembling materials. *Proc. Natl. Acad. Sci. U.S.A.* 2002; **99**: 5133–5138.

53 Kogiso M, Ohnishi S, Yase K, Masuda M, Shimizu T. Dicarboxylic oligopeptide bolaamphiphiles: proton-triggered self-assembly of microtubes with loose solid surfaces. *Langmuir* 1998; **14**: 4978–4986.

54 Seebach D, Overhand M, Kühnle FNM, Martinoni B, Oberer L, Hommel U, Widmer H. β-peptides: synthesis by Arndt-Eistert homologation with concomitant peptide coupling. Structure determination by NMR and CD spectroscopy and by X-ray crystallography. Helical secondary structure of a β-hexapeptide in solution and its stability towards pepsin. *Helv. Chim. Acta.* 1996; **79**: 913–941.

55 Thirunavukkuarasu S, Jares-Erijman EA, Jovin TM. Multiparametric fluorescence detection of early stages in the amyloid protein aggregation of pyrene-labeled α-synuclein. *J. Mol. Biol.* 2008; **378**: 1064–1073.

56 Giepmans BNG, Adams SR, Ellisman MH, Tsien RY. The fluorescent toolbox for assessing protein location and function. *Science* 2006; **312**: 217–224.

57 Jungbauer LM, Yu C, Laxton KJ, Ladu MJ. Preparation of fluorescently-labeled amyloid-beta peptide assemblies: the effect of fluorophore conjugation on structure and function. *J. Mol. Recognit.* 2009; **22**: 403–413.

58 LeVine III H. Thioflavine T interaction with amyloid β-sheet structures. *Amyloid* 1995; **2**: 1–6.

59 LeVine III H. Thioflavine T interaction with synthetic Alzheimer's disease β-amyloid peptides: detection of amyloid aggregation in solution. *Protein Sci.* 1993; **2**: 404–410.

60 Colombo G, Soto P, Gazit E. Peptide self-assembly at the nanoscale: a challenging target for computational and experimental biotechnology. *Trends Biotechnol.* 2007; **25**: 211–218.

61 Vauthey S, Santoso S, Gong H, Watson N, Zhang S. Molecular self-assembly of surfactant-like peptides to form nanotubes and nanovesicles. *Proc. Natl. Acad. Sci. U.S.A.* 2002; **99**: 5355–5360.

62 Stendahl JC, Rao MS, Guler MO, Stupp SI. Intermolecular forces in the self-assembly of peptide amphiphile nanofibers. *Adv. Funct. Mater.* 2006; **16**: 499–508.

63 Branco MC, Schneider JP. Self-assembling materials for therapeutic delivery. *Acta Biomater* 2009; **5**: 817–831.

64 Ghosh I, Chmielewski J. Peptide self-assembly as a model of proteins in the pre-genomic world. *Curr. Opin. Chem. Biol.* 2004; **8**: 640–644.

65 Motiei L, Rahimipour S, Thayer DA, Wong CH, Ghadiri MR. Antibacterial cyclic D,L-α-glycopeptides. *Chem. Commun.* 2009; **25**: 3693–3695.

66 Matsui H, Pan S, Gologan B, Jonas SH. Bolaamphiphile nanotube-templated metallized wires. *J. Phys. Chem. B.* 2000; **104**: 9576–9579.

67 Matsui H, Gologan B, Pan S, Douberly GE. Controlled immobilization of peptide nanotube-templated metallic wires on Au surfaces. *Eur. Phys. J. D.* 2001; **16**: 403–406.

68 Fraser PE, Nguyen JT, Surewicz WK, Kirschner DA. pH-dependent structural transitions of Alzheimer amyloid peptides. *Biophys. J.* 1991; **60**: 1190–1201.

69 Hardy J, Selkoe DJ. The amyloid hypothesis of Alzheimer's disease: progress and problems on the road to therapeutics *Science* 2002; **297**: 353–356.

70 Soto C. Estrada LD. Protein misfolding and neurodegeneration. *Arch. Neurol.* 2008; **65**: 184–189.

71 Soto C. Unfolding the role of protein misfolding in neurodegenerative diseases. *Nature Rev. Neurosci.* 2003; **4**: 49–60.

72 Fezoui Y, Teplow DB. Kinetic studies of amyloid β-protein fibril assembly. Differential effects of α-helix stabilization. *J. Biol. Chem.* 2002; **277**: 36948–36954.

73 Khurana R, Coleman C, Ionescu-Zanetti C, Carter SA, Krishna V, Grover RK, Roy R, Singh S. Mechanism of thioflavin T binding to amyloid fibrils. *J. Struct. Biol.* 2005; **151**: 229–238.

74 Wiltfang J, Esselmann H, Cupers P, Neumann M, Kretzschmar H, Beyermann M, Schleuder D, Jahn H, Rüther E, Kornhuber J, Annaert W, De Strooper B, Saftig P. Elevation of β-amyloid peptide 2–42 in sporadic and familial Alzheimer's Disease and its generation in PS1 knockout cells. *J. Biol. Chem.* 2001; **276**: 42645–42657.

